

COHERENCE PROPERTIES OF THE ODD HARMONICS OF THE RADIATION FROM SASE FEL WITH PLANAR UNDULATOR

E.A. Schneidmiller, M.V. Yurkov, DESY, Hamburg, Germany

Abstract

We present analysis of coherence properties of odd harmonics radiated from a SASE FEL with planar undulator. Nonlinear mechanism of harmonic generation is under study. Temporal and space correlation functions, coherence time and degree of transverse coherence are calculated by means of numerical simulations with the code FAST. Similarity techniques have been used to derive general coherence properties of the radiation from optimized x-ray FEL operating in the saturation regime.

INTRODUCTION

We consider free electron laser (FEL) amplifier - device in which electron bunch amplifies electromagnetic radiation during single pass of an undulator. The FEL collective instability in the electron beam produces an exponential growth (along the undulator) of the radiation and the modulation of the electron density on the scale of undulator resonance radiation wavelength. Amplification process in a Self Amplified Spontaneous Emission (SASE) FEL [1] starts from the shot noise in the electron beam. When the electron beam enters the undulator, the presence of the beam modulation at frequencies close to the resonance frequency initiates the process of radiation. The fluctuations of current density in the electron beam are uncorrelated not only in time but in space, too. A big number of transverse mode is excited. TEM₀₀ mode with highest gain dominates when undulator length progresses. Coherence time and degree of transverse coherence grow in the exponential amplification stage, and reach maximum values near the saturation point. Saturation length is limited from nine to eleven field gain length for VUV and x-ray FELs which fundamentally define coherence properties of the radiation [2–6]. Poor longitudinal coherence also affects transverse coherence [2, 3].

Radiation from SASE FEL with planar undulator contains visible contribution of odd harmonics. Parameter range where intensity of higher harmonics is defined mainly by nonlinear beam bunching in the fundamental harmonic has been intensively studied in refs. [7–16]. Comprehensive studies of nonlinear harmonic generation have been performed in [16] in the framework of the one-dimensional model. General features of harmonic radiation have been determined. It was found that coherence time at saturation falls inversely proportional to harmonic number, and relative spectrum bandwidth remains constant with harmonic number. In this paper we extend studies of higher harmonics taking into account diffraction effects. We consider parameter range when intensity of higher harmonics is mainly defined by nonlinear harmonics gener-

ation mechanism. The results have been obtained with time-dependent, three-dimensional FEL simulation code FAST [17] performing simulation of the FEL process with actual number of electrons in the beam. Using similarity techniques we present universal dependencies for the main characteristics of the SASE FEL covering all practical range of optimized X-ray FELs. Present studies are limited with the third harmonic.

OPTIMIZED XFEL

Design of the focusing system of XFEL assumes nearly uniform focusing of the electron beam in the undulator, so we consider axisymmetric model of the electron beam. It is assumed that transverse distribution function of the electron beam is Gaussian, so rms transverse size of matched beam is $\sigma = \sqrt{\epsilon\beta}$, where $\epsilon = \epsilon_n/\gamma$ is rms beam emittance and β is focusing beta-function. In the case of negligibly small effects of the space charge and energy spread, operation of the FEL amplifier is described by the diffraction parameter B and the betatron motion parameter \hat{k}_β : [18]:

$$B = 2\Gamma\sigma^2\omega/c, \quad \hat{k}_\beta = 1/(\beta\Gamma), \quad (1)$$

where $\Gamma = [I\omega^2\theta_s^2 A_{JJ1}^2 / (I_A c^2 \gamma_z^2 \gamma)]^{1/2}$ is the gain parameter. When describing shot noise in the electron beam, one more parameter appears, the number of electrons in the volume of coherence: $N_c = I/(e\omega\rho)$, where $\rho = c\gamma_z^2\Gamma/\omega$ is the efficiency parameter. The following notations are used here: I is the beam current, $\omega = 2\pi c/\lambda$ is the frequency of the electromagnetic wave, $\theta_s = K_{rms}/\gamma$, K_{rms} is the rms undulator parameter, γ is relativistic factor, $\gamma_z^{-2} = \gamma^{-2} + \theta_s^2$, $k_w = 2\pi/\lambda_w$ is the undulator wavenumber, $I_A = 17$ kA is the Alfvén current. Coupling factor is $A_{JJ1} = 1$ for helical undulator and $A_{JJh} = J_{(h-1)/2}(K_{rms}^2/2(1 + K_{rms}^2)) - J_{(h-1)/2}(K_{rms}^2/2(1 + K_{rms}^2))$ for planar undulator. Here J_n are the Bessel functions of the first kind, and h is harmonic number.

Target value of interest for XFEL optimization is the field gain length of the fundamental mode. For this practically important case the solution of the eigenvalue equation for the field gain length of the fundamental mode and optimum beta function are rather accurately approximated by [19]:

$$L_g = 1.67 \left(\frac{I_A}{I}\right)^{1/2} \frac{(\epsilon_n \lambda_w)^{5/6}}{\lambda^{2/3}} \frac{(1 + K^2)^{1/3}}{K A_{JJ1}}$$

$$\beta_{opt} \simeq 11.2 \left(\frac{I_A}{I}\right)^{1/2} \frac{\epsilon_n^{3/2} \lambda_w^{1/2}}{\lambda K A_{JJ1}}, \quad (2)$$

It follows from (1) and (2) that diffraction parameter B and parameter of betatron oscillations, \hat{k}_β are functions of the

ISBN 978-3-95450-123-6

only parameter $\hat{\epsilon}$ for optimized x-ray FEL. As a result, saturation characteristics of the SASE FEL written down in the dimensionless form are functions of two parameters, $\hat{\epsilon}$ and parameter N_c defining the initial conditions for the start-up from the shot noise [3–5]. Dependence of characteristics on the value of N_c is very slow, in fact logarithmic. Properties of the third harmonic are also function of emittance parameter $\hat{\epsilon}$. In the case when mechanism of nonlinear harmonic generation is dominating, dependencies on the coupling factor can be explicitly isolated. This property provides the possibility of universal description of characteristics of higher harmonics.

GENERAL DEFINITIONS

The first-order transverse correlation function is defined as

$$\gamma_1(\vec{r}_\perp, \vec{r}'_\perp, z, t) = \frac{\langle \tilde{E}(\vec{r}_\perp, z, t) \tilde{E}^*(\vec{r}'_\perp, z, t) \rangle}{\left[\langle |\tilde{E}(\vec{r}_\perp, z, t)|^2 \rangle \langle |\tilde{E}(\vec{r}'_\perp, z, t)|^2 \rangle \right]^{1/2}},$$

where \tilde{E} is the slowly varying amplitude of the amplified wave. For a stationary random process γ_1 does not depend on time, and the degree of transverse is:

$$\zeta = \frac{\int |\gamma_1(\vec{r}_\perp, \vec{r}'_\perp)|^2 I(\vec{r}_\perp) I(\vec{r}'_\perp) d\vec{r}_\perp d\vec{r}'_\perp}{\left[\int I(\vec{r}_\perp) d\vec{r}_\perp \right]^2}, \quad (3)$$

where $I(\vec{r}_\perp) = \langle |\tilde{E}(\vec{r}_\perp)|^2 \rangle$. The first order time correlation function, $g_1(t, t')$, is calculated in accordance with the definition:

$$g_1(\vec{r}, t - t') = \frac{\langle \tilde{E}(\vec{r}, t) \tilde{E}^*(\vec{r}, t') \rangle}{\left[\langle |\tilde{E}(\vec{r}, t)|^2 \rangle \langle |\tilde{E}(\vec{r}, t')|^2 \rangle \right]^{1/2}}, \quad (4)$$

For a stationary random process time correlation functions are functions of the only argument, $\tau = t - t'$. The coherence time is defined as $\tau_c = \int_{-\infty}^{\infty} |g_1(\tau)|^2 d\tau$. Normalized coherence time is defined as $\hat{\tau}_c = \rho \omega \tau_c$. Normalized FEL efficiency is defined as $\hat{\eta} = P / (\rho W_b)$ where P is radiation power, and $W_b = \gamma m c^2 I / e$ is electron beam power. If one traces evolution of the brilliance of the radiation along the undulator length there is always the point, which we define as the saturation point, where the brilliance reaches maximum value [3].

PROPERTIES OF THE RADIATION

Simulations have been performed with three-dimensional, time-dependent FEL simulation code [17] tracing actual number of electrons. In our simulation procedure particles correspond to real electrons randomly distributed in full 6D phase space. This allows us to avoid any artificial effects arising from standard procedures of macroparticle loading as we described earlier [3]. Simulations of the FEL process have been performed for the case of a long bunch with uniform axial profile of

the beam current. Such a model provides rather accurate predictions for the coherence properties of the XFEL, since typical radiation pulse from the XFEL is much longer than the coherence time. Calculations has been performed with FEL simulation code FAST using actual number of electrons in the beam. The value of parameter $N_c = 8 \times 10^5$ corresponds to the parameter range of XFEL operating at the radiation wavelength about 0.1 nm. Simulated range covers the value of emittance parameter $\hat{\epsilon}$ from 0.25 to 2.

Output of the simulation code are arrays containing complex values of the radiation field amplitudes. Then we apply statistical analysis, and calculate physical values as it has been defined in the previous section. Finally, application of similarity techniques allows us to extract universal parametric dependencies of the main characteristics of the optimized XFEL.

We start with specific numerical example corresponding to the value of $\hat{\epsilon} = 0.5$. This operating point correspond to maximum degree of transverse coherence which can be achieved in SASE FEL [3, 5, 6]. Figure 1 shows slice of temporal structure of the radiation pulse from SASE FEL operating in the saturation regime. Already this specific example brings a lot of physical information. We note that spikes of all harmonics are well aligned in space illustrating an effect of nonlinear harmonic generation: higher harmonics radiate only by those parts of the electron bunch which has been effectively modulated by the fundamental harmonic. We also notice that typical scale of the radiation intensities of the 3rd (5th) harmonic is in the range of a per cent (per mille) level with respect to the fundamental. Even brief look on spike widths in Fig. 1 gives us an idea that coherence time of the 3rd harmonic is significantly less than that of the fundamental harmonic. Spikes of the 5th harmonics are shorter than those of the 3rd harmonics, thus coherence time of the 5th harmonic should be even less.

Plots in Fig. 2 show evolution along the undulator of the radiation power and brilliance. Longitudinal coordinate is normalized to the saturation length of the fundamental har-

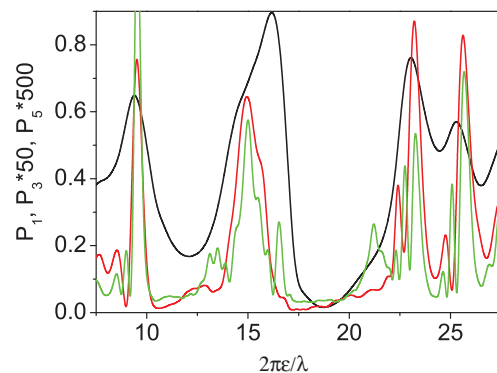


Figure 1: Optimized XFEL. Temporal structure of the radiation pulse in the saturation point for $\hat{\epsilon} = 0.5$. Black, red, and green lines refer to the 1st, 3rd, and 5th harmonic, respectively.

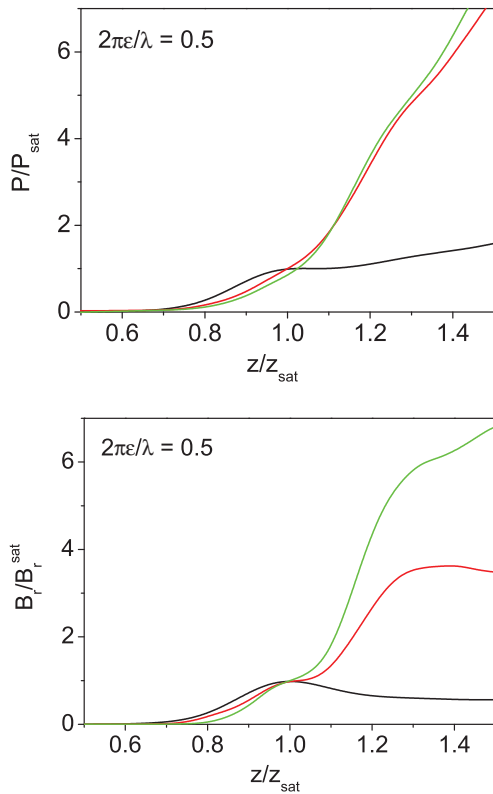


Figure 2: Optimized XFEL. FEL power and brilliance versus undulator length. All values are normalized to the values corresponding to the values at the saturation point of the fundamental harmonic. Black, red, and green lines refer to the 1st, 3rd, and 5th harmonic, respectively.

monic. Brilliance and power for harmonics are normalized to the values corresponding to the saturation point of the fundamental harmonic. We see that radiation powers of all harmonics continue to grow after the saturation point of the fundamental harmonic. Power growth of the 3rd and the 5th harmonic is visibly faster than that of the fundamental. An important feature is also that brilliance of the higher harmonics continue to grow as well after the saturation point. Maximum brilliance of the higher harmonics is reached in the deep nonlinear regime which is mainly due to faster growth of the harmonic radiation power with respect to the fundamental. This means that in parameter range of $\hat{\epsilon}$ about 0.5 electron beam after saturation remains relatively good amplification media for higher harmonics. Contribution of higher harmonics into total radiation power depends strongly on how long amplification process develops after the saturation point.

Plots in Fig. 3 show evolution along the undulator of the coherence time and degree of transverse coherence. We multiplied coherence time by harmonic number h to bring all curves into scale. We find important feature that coherence time in the saturation regime scales inversely proportional to harmonic number. Also, relative spectrum bandwidth $\Delta\omega_h/\omega_h$ remains constant for all harmonics. This finding confirms the result obtained earlier in the frame-

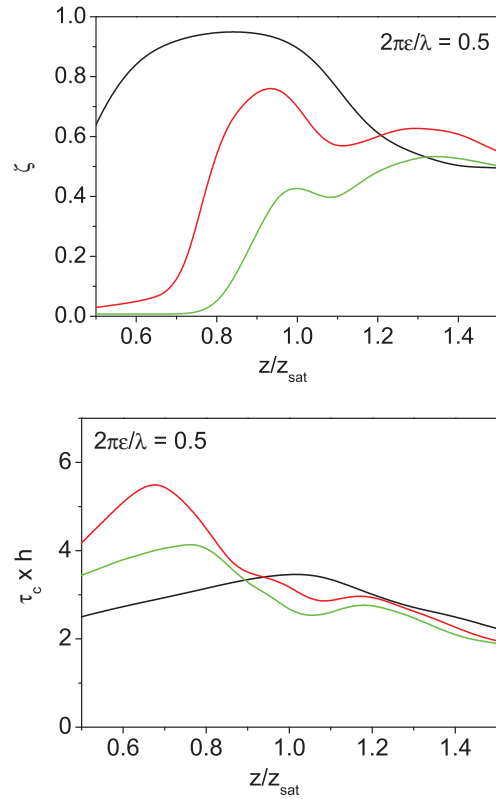


Figure 3: Optimized XFEL. Degree of transverse coherence, ζ , and normalized coherence time, $\hat{\tau}_c$ versus undulator length for $\hat{\epsilon} = 0.5$. Black, red and green lines refer to the 1st, 3rd and 5th harmonic, respectively. Coherence time is multiplied for corresponding harmonic number h .

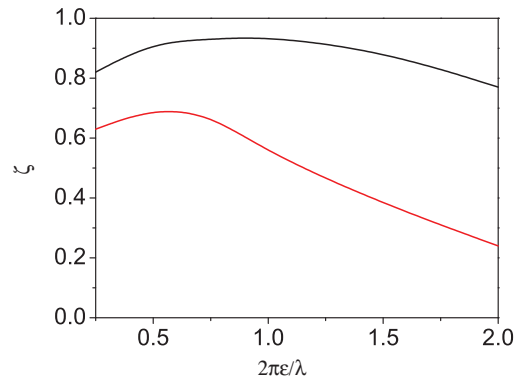


Figure 4: Optimized XFEL. Degree of transverse coherence ζ_{sat} in the saturation versus parameter $\hat{\epsilon} = 2\pi\epsilon/\lambda$. Black and red lines refer to the 1st, 3rd harmonic, respectively.

work of one dimensional model [16]. Note that recent measurements of the harmonic properties at FLASH and LCLS [20, 21] are in good qualitative agreement with the results reported here.

Figure 2 shows evolution of the degree of transverse coherence along the undulator. Note that we illustrate parameter space providing maximum degree of transverse coher-

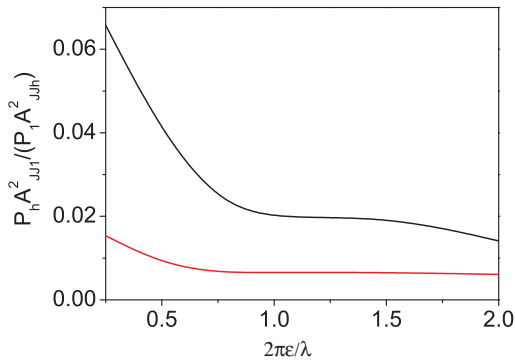


Figure 5: Optimized XFEL. Ratio of powers in the 3rd (black line) and the 5th harmonic (red line) to the power of the fundamental harmonic versus parameter $\epsilon = 2\pi\epsilon/\lambda$. SASE FEL operates at the saturation point.

ence in the fundamental harmonic (about 95%) for optimized x-ray FEL. An important observation is that the degree of transverse coherence for higher harmonics is visibly less. There is nothing unusual in this result. Qualitatively it can be explained by general feature of frequency multiplication schemes which also amplify noise progressively with harmonic number [22]. Fundamental harmonic already contains visible noise content resulting in reduced degree of transverse coherence, and we can readily expect more reduction for higher harmonics. An example of similar physical behavior is degradation of longitudinal coherence in high gain harmonic generation scheme [23].

As we already mentioned above, characteristics of the optimized FEL in the saturation point depend on the only parameter, $\hat{\epsilon}$. Figure 4 shows dependence of the degree of transverse coherence for the 1st and the 3rd harmonic on the value of emittance parameter. We see that maximum values of the degree of transverse coherence correspond to the values of $\hat{\epsilon}$ about 0.5. While coherence properties of the fundamental harmonic do not change too much when $\hat{\epsilon}$ increases to 2, we obtain their significant degradation for the 3rd harmonic.

When we analyze expressions for the radiation power we find that the dependencies for the ratios of the power of higher harmonics to the fundamental become to be universal functions of emittance parameter when we factorize them with factor A_{JJh}^2/A_{JJ1}^2 . Relevant plots are presented in Fig. 5. For large values of the undulator parameter K asymptotic values of A_{JJh}^2/A_{JJ1}^2 are equal to 0.22 and 0.11 for the 3rd and the 5th harmonic, respectively. In the range of emittance parameter from 0.25 to 2 contributions to the total power of the 3rd (5th) harmonic is between 0.3 - 1.4% (0.07 - 0.16%). Note that contribution of higher harmonics to the total power grows in the deep nonlinear regime, and may constitute substantial amount (See Fig. 2).

ISBN 978-3-95450-123-6

SUMMARY

In conclusion we make brief summary of our findings related to the saturation regime. Degree of transverse coherence of higher harmonics is less than that of the fundamental. Coherence time for harmonics scales inversely proportional to the harmonic number. Relative width of the radiation spectrum is the same for all harmonics.

REFERENCES

- [1] Ya.S. Derbenev, A.M. Kondratenko and E.L. Saldin, Nucl. Instrum. and Methods **193**(1982)415.
- [2] E.L. Saldin, E.A. Schneidmiller, and M.V. Yurkov, Opt. Commun. **186**(2000)185.
- [3] E.L. Saldin, E.A. Schneidmiller, and M.V. Yurkov, Opt. Commun. 281(2008)1179.
- [4] E.L. Saldin, E.A. Schneidmiller, and M.V. Yurkov, Opt. Commun. 281(2008)4727.
- [5] E.L. Saldin, E.A. Schneidmiller, and M.V. Yurkov, New J. Phys. 12 (2010) 035010, doi: 10.1088/1367-2630/12/3/035010.
- [6] G.Geloni et al., New J. Phys. 12 (2010) 035021, doi: 10.1088/1367-2630/12/3/035021.
- [7] M. Schmitt and C. Elliot, Phys. Rev. A, 34(1986)6.
- [8] R. Bonifacio, L. De Salvo, and P. Pierini, Nucl. Instr. Meth. A 293(1990)627.
- [9] W.M. Fawley, Proc. IEEE Part. Acc. Conf., 1995, p.219.
- [10] H. Freund, S. Biedron and S. Milton, Nucl. Instr. Meth. A 445(2000)53.
- [11] H. Freund, S. Biedron and S. Milton, IEEE J. Quant. Electr. 36(2000)275.
- [12] S. Biedron et al., Nucl. Instr. Meth. A 483(2002)94.
- [13] S. Biedron et al., Phys. Rev. ST 5(2002)030701.
- [14] Z. Huang and K. Kim, Phys. Rev. E, 62(2000)7295.
- [15] Z. Huang and K. Kim, Nucl. Instr. Meth. A 475(2001)112.
- [16] E.L. Saldin, E.A. Schneidmiller and M.V. Yurkov, Phys. Rev. ST-AB 9(2006)030702
- [17] E.L. Saldin, E.A. Schneidmiller, and M.V. Yurkov, Nucl. Instrum. and Methods **A 429**(1999)233.
- [18] E.L. Saldin, E.A. Schneidmiller and M.V. Yurkov, Nucl. Instrum. and Methods **A475**(2001)86.
- [19] E.L. Saldin, E. A. Schneidmiller, and M.V. Yurkov, Opt. Commun. 235(2004)415.
- [20] W. Ackermann et al., Nature Photonics **1**(2007)336
- [21] D. Ratner et al., Phys. Rev. ST-AB 14(2011)060701
- [22] W. P. Robins, Phase noise in signal sources (IEE Telecommunications series 9, Peter Peregrinus Ltd, 1982).
- [23] E.L. Saldin, E. A. Schneidmiller, and M.V. Yurkov, Opt. Commun. 202(2002)169.